https://doi.org/10.1070/RCR4944

Tuning the dihydroazulene – vinylheptafulvene couple for storage of solar energy

Mogens Brøndsted Nielsen,[a]* Nicolai Ree,[a] Kurt V. Mikkelsen,[a]* Martina Cacciarini [b]*

[a] Department of Chemistry, University of Copenhagen, Universitetsparken 5, DK-2100 Copenhagen Ø, Denmark
[b] Department of Chemistry, University of Florence, via della Lastruccia 3-13, 50019 Sesto F. No (FI), Italy

Dihydroazulene (DHA) is a molecular photoswitch that undergoes a ring-opening reaction upon irradiation to form a vinylheptafulvene (VHF) photoisomer. This VHF isomer will in time thermally return to the DHA isomer. As the isomerization is photo-induced only in one direction, the DHA – VHF couple has attracted interest as a molecular solar thermal energy storage device (MOST system). In this author review, we cover our systematic efforts to optimize the DHA – VHF couple for this purpose, with challenges being to achieve sufficiently high energy densities, to cover broad absorptions including the visible region, and to control the energy-releasing VHF-to-DHA back-reaction. By a combination of computations and experiments, we review the consequences of various structural modifications of the system (structure – property relationships), including the influence of donor-acceptor substitution at specific positions, benzannulations, and incorporation into macrocyclic structures. Synthetic protocols to reach the various modifications will also be discussed. The bibliography includes 60 references.

Contents

1. Introduction 573
2. Dihydroazulene-to-vinylheptafulvene photoisomerization 575
3. Vinylheptafulvene-to-dihydroazulene back-reaction 576
4. Cyclability studies 576
5. Chemically induced transformations: DHA-to-VHF and VHF-to-DHA 577
6. Dihydroazulene synthesis 577
7. Computational screenings: towards high energy densities 578
8. Functionalization at position C(2) 579
9. Functionalization at position C(3) 580
10. Functionalization at position C(7) 580
11. Replacing one cyano group at position C(1) 581
12. Benzannulation of the five-membered ring 582
13. Benzannulation of the seven-membered ring 582
14. Macrocyclic structures 583
15. Dihydroazulene — norbornadiene conjugates 585
16. Conclusion 585

M.B.Nielsen. PhD, Dr. Scient. in Chemistry, Professor of Organic Chemistry at the Department of Chemistry, University of Copenhagen
E-mail: mbn@chem.ku.dk
N.Ree. PhD student in theoretical chemistry at the same University.
E-mail: nree@chem.ku.dk
K.V.Mikkelsen. PhD, Dr. Scient. in Chemistry, Professor of Theoretical Chemistry at the same University. E-mail: kmi@chem.ku.dk
M.Cacciarini. PhD in Chemistry, Associate Professor in Organic Chemistry at the Department of Chemistry, University of Florence.
E-mail: martina.cacciarini@unifi.it
Current research interests of the authors: development of photochromic molecules for storage of solar energy.

1. Introduction

In the last 50 years, the global emissions of anthropogenic greenhouse gases have almost doubled due to the rapidly growing population and an ever increasing need for food, natural resources, and energy.[1–3] As a consequence, the global mean surface temperature has increased by approximately 0.8 °C leading to climate changes with devastating ecological, physical, and health impacts. A global effort to reduce the emissions of greenhouse gases is crucial, which urges for an ambitious and fast transition to renewable energy sources. A report from March 2019 showed that 74% of the existing coal-fired power plants in the USA could be replaced by wind or solar energy with the result of

Received 22 January 2020
© 2020 Uspekhi Khimii, ZIOC RAS, Russian Academy of Sciences and IOP Publishing Limited

an immediate profit.[4] Yet, a major obstacle to the global energy transition is not to produce clean energy, but rather to sustain a stable and safe electricity grid that matches the immediate power demands of the consumers.[5,6] The daily and seasonal variations in the production of renewable energy and the large variations in the power demands are two serious challenges for the electricity supply, which could be solved if excess power was stored and used in peak times. Energy storage systems are, therefore, crucial for the global transition to a sustainable future.

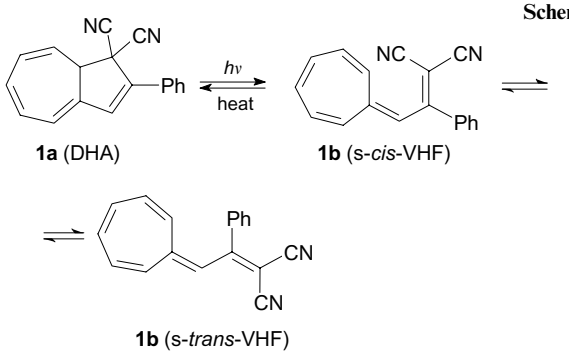
Looking at the total energy consumption, heating and cooling accounted for 51% of the final energy use in 2016, while transport and electricity demand (excluding the purposes of heating, cooling, and transport) accounted for 32% and 17%, respectively.[7] Heating and cooling are therefore the main contributors to the global energy consumption. Unfortunately, only 10% of the energy consumption for heating and cooling can be assigned to renewable energy sources, while over a quarter of the electricity demand is produced by renewable energy sources. Furthermore, heating and cooling energy from renewable energy sources grew by only 5% in the period from 2013 to 2017, while the production of renewable electricity increased by 25%.[7] Hence, most of the global energy-related emissions of greenhouse gases are caused by heating and cooling, which calls for significant changes to reduce the climate footprint of this sector. One technology that attempts to solve this problem and to create a solution for energy storage is closed-cycle MOlecular Solar Thermal (MOST) systems or MOST batteries based on photochromic molecules.[8–17] Such systems use solar radiation to drive thermodynamically unfavourable isomerization reactions of stable reactants to metastable products through photoexcitation and excited state processes. Thus, the energy is stored as chemical energy until a subsequent exothermic reaction releases the captured solar energy without any exchange of matter.

The energy release can either occur spontaneously or be controlled by a thermal activation, a heterogeneous catalyst, an electric potential, or light, depending on the storage lifetime. In other words, MOST systems are capable of harvesting and storing solar energy, which can later be released as clean thermal energy for space heating or heating of domestic water. But most importantly, the thermal energy can be stored without the need for thermal insulation, which enables prolonged storage times compared to alternative thermal energy storage systems. The MOST systems are based on photochemically active compounds known as photochromic molecules or molecular photoswitches, which are able to interconvert through either a *cis*–*trans* isomerization, a dimerization, an organometallic rearrangement, or an electrocyclic reaction.

An ideal MOST system would absorb visible light with a quantum yield of photoisomerization of 100%, have an energy density of 1 MJ kg^{-1} (comparable to Li-ion batteries), have a back-reaction that is completely on hold until triggered by a suitable stimulus, be water-soluble for flow system applications, suffer from no photodegradation thereby allowing for an infinite number of cycles, and be easily synthesized at low cost and with no heavy metals involved. Finding one system satisfying all these criteria is, however, a challenging task. Several molecules have been moved forward for MOST applications and optimized in some of the respects,[8–17] such as *cis*–*trans* isomeric azobenzenes,[14] the norbornadiene–quadricyclane (NBD–QC) couple,[8,9] (fulvalene)tetracarbonyldiruthenium compounds,[10] 1,2-dihydro-1,2-azaborinine and its Dewar valence isomer,[15] the dithienylethene–dihydrobenzodithiophene couple,[17] and the dihydroazulene–vinylheptafulvene (DHA–VHF) couple. This review will focus on the dihydroazulene–vinylheptafulvene couple, and it will cover the efforts that have been spent in the past decade to tune properties towards MOST applications. In particular, we will concentrate on how structural modifications alter the energy storage capacity and the half-life of the energy release reaction.

When referring to the parent structure of DHA, we will consider the structure **1a** shown in Scheme 1, which contains two cyano groups at C(1) and a phenyl group at C(2) atoms (for azulene numbering, see Fig. 1). The compound has a stereocentre at C(8a) and hence exists as a pair of enantiomers. It was first prepared by Daub *et al.*[18] and found to undergo photoisomerization to the corresponding VHF (**1b**). This isomerization is accompanied by significant changes in the UV-Vis absorption spectra: DHA (**1a**) has a characteristic absorption at 353 nm, while VHF (**1b**) has a characteristic absorption at 470 nm in acetonitrile (Fig. 2).[19,20] Vinylheptafulvene (**1b**) is in equilibrium between s-*cis* and s-*trans* conformers; the latter is usually the most stable, while the former is required for the thermal back-reaction, regenerating DHA. By being only photoactive in one direction, DHA can be fully photoisomerized into VHF (no photostationary state), and in the dark DHA will be fully regenerated in time, which renders the system attractive for MOST applications.

Scheme 1



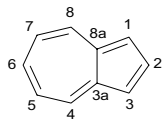


Figure 1. Numbering of azulene.

In general, we will use the labels **a** and **b** to designate a couple of DHA and VHF isomers. For simplicity, we will ignore in the labelling that, in some cases, the DHA and VHF forms can exist as mixtures of diastereoisomers (when two different groups are located at the C(1) atom of DHA instead of two identical cyano groups).

The following designations and abbreviations are used:

Ac — acetyl,

a.u. — arbitrary units,

B3LYP — Becke, 3-parameter, Lee–Yang–Paar exchange-correlation functional,

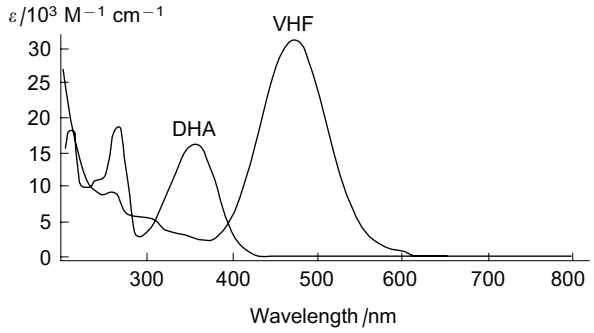


Figure 2. UV-Vis absorption spectra of DHA (**1a**) and VHF (**1b**) in MeCN.[20] ε is molar absorptivity.

BrettPhos — 2-(dicyclohexylphosphino)-3,6-dimethoxy-2′,4′,6′-triisopropyl-1,1′-biphenyl,
CAM — Coulomb-attenuating method,
Cy — cyclohexyl,
DDQ — 2,3-dichloro-5,6-dicyano-1,4-benzoquinone,
DFT — density functional theory,
DHA — dihydroazulene,
DIBAL-H — diisobutylaluminium hydride,
DMAP — *N*,*N*-dimethyl-4-aminopyridine,
ε — molar absorptivity,
EDG — electron-donating group
$E_T(30)$ — Dimroth – Reichardt solvent parameter,
EWG — electron-withdrawing group,
HMDS — hexamethyldisilazane,
IEF-PCM — integral equation formalism version of the polarizable continuum model,
k — rate constant,
k_{subst} — rate constant for substituted derivative,
k_H — rate constant for unsubstituted derivative,
LiHMDS — lithium hexamethyldisilazide,
LN — lithium naphthalenide,
M06-2X — Minnesota global hybrid functional with 54% HF exchange,
MOST — molecular solar thermal,
NBD — norbornadiene,
NBS — *N*-bromosuccinimide,
Py — pyridine,
QC — quadricyclane,
RuPhos — 2-dicyclohexylphosphino-2′,6′-diisopropoxy-biphenyl,
σ_{subst} — Hammett substituent constant,
$\sigma_{m,R}$ — Hammett substituent constant for *meta* substiuent R,
$\sigma_{p,R}$ — Hammett substituent constant for *para* substiuent R,
S_0 — singlet ground state,
S_1 — first excited singlet state,
$t_{1/2}$ — half-life,
TBDMS — *tert*-butyldimethylsilyl,
TFA — trifluoroacetic acid,
Ts — tosyl,
TS — transition state,
UV — ultraviolet,
VHF — vinylheptafulvene,
Vis — visible.

2. Dihydroazulene-to-vinylheptafulvene photoisomerization

The DHA-to-VHF photoisomerization occurs with a relatively high quantum yield, being, however, somewhat solvent dependent; for the photoisomerization of DHA (**1a**) into VHF (**1b**), it is 0.35% in methylcyclohexane, 60% in toluene, 50% in ethanol, and 55% in acetonitrile.[21] The mechanism of the photoinduced ring-opening reaction was studied in detail in a recent computational study,[22] where the phenyl substituent was replaced by a hydrogen atom. The results show that planarization plays a crucial role for the carbon – carbon bond-breaking and, hence, for ring-opening, of the excited DHA (**1a**). Upon photoexcitation, the planarization was found to occur within 300 – 500 fs, leading to ring-opening and concurrent decay of the molecule to the VHF (**1b**) ground state within 100 fs through an $S_1 \rightarrow S_0$ internal conversion process (S_0 and S_1 are the ground and first excited singlet states). These theoretical results are in agreement with ultrafast time-resolved experiments.[23] The reaction path with structural alterations is

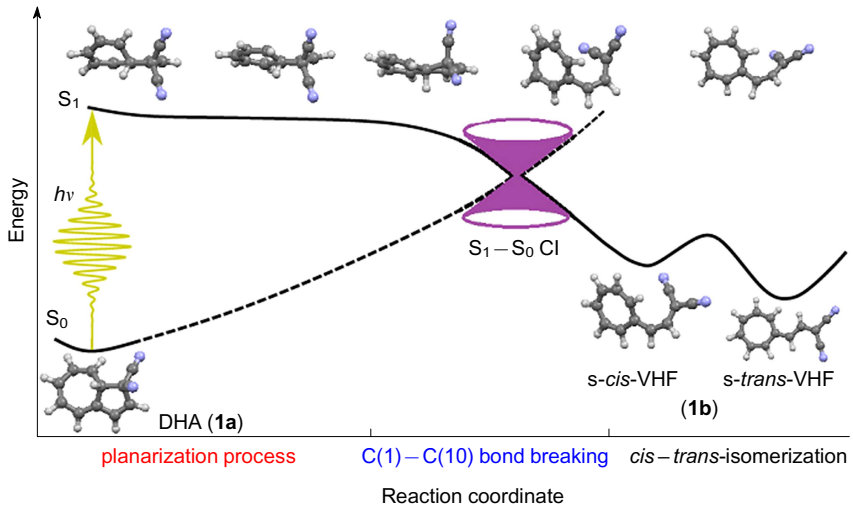


Figure 3. Schematic illustration of the reaction path from DHA (**1a**) to VHF (**1b**) upon photoexcitation (the phenyl group at C(2) of **1a** is here replaced by H).[22] S_0 and S_1 are the ground and first excited singlet states, CI is $S_1 - S_0$ conical intersection.

shown in Fig. 3. The interconversion between s-*cis* and s-*trans* conformers occurs on subpicosecond time scale.

3. Vinylheptafulvene-to-dihydroazulene back-reaction

The thermal VHF-to-DHA back-reaction occurs for **1b** in acetonitrile at 25 °C with a half-life of 208 – 218 min.[19] The rate was, however, found to be strongly solvent-dependent, being higher in polar solvents.[19,24] Thus, a linear empirical relationship between $\ln k$ (where k is the rate constant for the reaction at 25 °C) and the Dimroth – Reichardt $E_T(30)$ solvent parameter was obtained as shown in Fig. 4.[19] This result calls for a polar transition state in the ring closure reaction in line with theoretical studies.[23,25–29] Transition state calculations for the ring closure of **1b** show that both the disrotatory (Woodward – Hoffmann allowed) and the conrotatory pathways are influenced by solvent polarity, with reaction barriers decreasing in both cases with solvent polarity.[29] In the case of **1b**, the conrotatory pathway has the lowest barrier in all solvents; instead, replacement of one nitrile for other groups changes the relative stability of the transition states, suggesting that two competing pathways are possible. NMR spectroscopic studies in different solvents of the ring closure of VHF derivative **2b** into DHA diastereoisomers **2a** and **2a′** (Scheme 2) convincingly supported the calculations.[29] Thus, the ratio between the two diastereoisomers [having stereocentres at C(1) and C(8a) atoms] was found to vary with solvent polarity, corresponding to ring closures by either conrotatory or disrotatory modes.

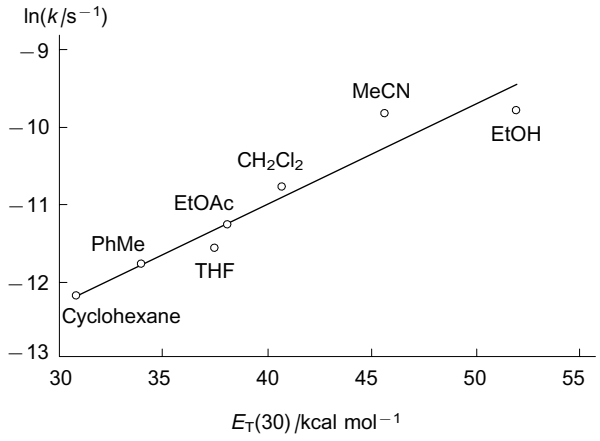
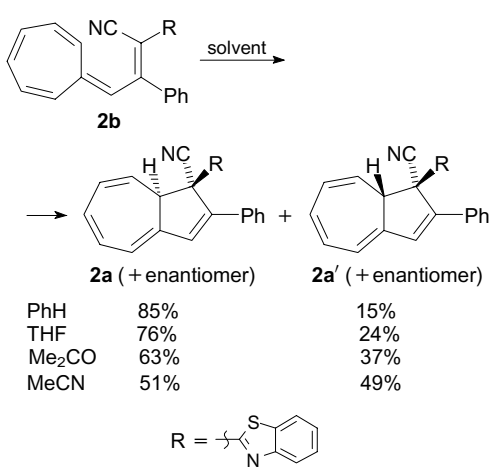


Figure 4. Relationship between natural logarithm of rate constant k (at 25 °C) for VHF-to-DHA conversion and solvent polarity.[19] $E_T(30)$ is the Dimroth – Reichardt solvent parameter. The best straight line describing the data is given.

A polarized transition state was further supported by the fact that the rate of VHF-to-DHA conversion is strongly tuned by electron-donating groups (EDGs) and electron-withdrawing groups (EWGs) at specific positions on the core.[30–33] In fact, Hammett correlations were established for substituent groups at positions C(2), C(3), and C(7) when plotting $\ln k$ (where k is the rate constant for the ring closure reaction) against the Hammett substituent constant σ. The signs of the slopes and hence the dependency on donor or acceptor character are summarized in

Scheme 2



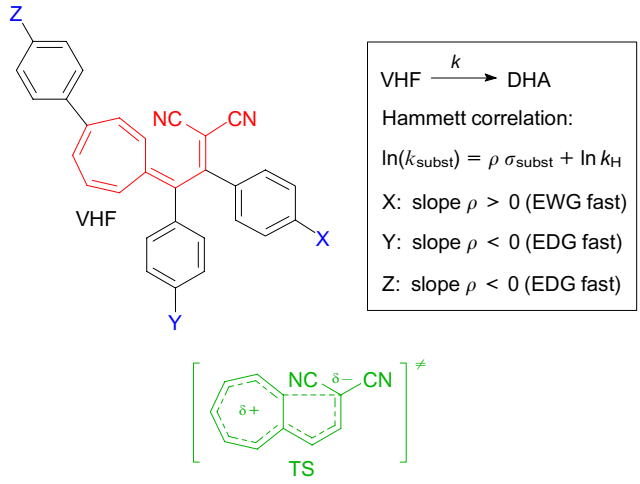


Figure 5. Summary of substituent influences on the VHF (**1b**) ring closure; Hammett correlations were obtained for structural variations at positions C(2), C(3), and C(7). The signs of the slopes (ρ) are listed in the box. k_{subst} is the rate constant for substituted derivative; k_H is the rate constant for unsubstituted derivative (X, Y, or Z = H); σ_{subst} is the Hammett substinuent constant. A suggested transition state (TS) structure of zwitterionic character is shown for the ring closure reaction.

Fig. 5. Examples of these tunings of the back-reaction by functional groups will be covered below. A suggested transition state (TS) structure is also shown in Figure 5.

Recently a Hammett correlation was established also for a small selection of C(1)-substituted DHAs (see below).[34]

4. Cyclability studies

The stability of **1a** – **1b** couple was investigated by subjecting it to photothermal cycles in various solvents.[35] The characteristic VHF (**1b**) absorbance at 460 nm was used to follow the conversions. The studies revealed less than 0.01% degradation per cycle in toluene (Fig. 6) and hence very high stability in this solvent. A faster degradation was observed in polar solvents, with around 0.28% and 0.18% loss of absorbance per cycle in ethanol and acetonitrile, respectively. One degradation channel seems to be the formation of fully unsaturated azulene derivatives [by

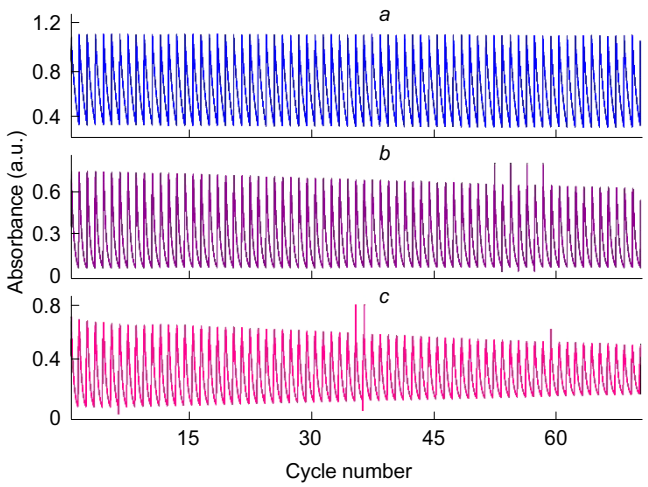


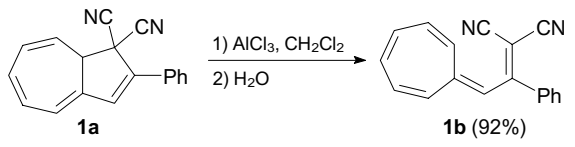
Figure 6. Cyclability test of DHA – VHF conversions using the VHF absorbance at 460 nm in toluene, *ca.* 10^{-4} mol L^{-1} (*a*), acetonitrile, *ca.* 10^{-4} mol L^{-1} (*b*), and ethanol, *ca.* 10^{-4} mol L^{-1} (*c*). The experiments were performed at a constant temperature of 60 °C, and 365 nm light was repeatedly switched on and off. One cycle includes one light-on period and one light-off period. Parasitic signals (spikes) appear in acetonitrile and ethanol and originate from instrumental fluctuations.[35] The abbreviation a.u. represents arbitrary units.

elimination of HCN at the C(1) – C(8a) bond] according to mass spectrometric analysis.

5. Chemically induced transformations: DHA-to-VHF and VHF-to-DHA

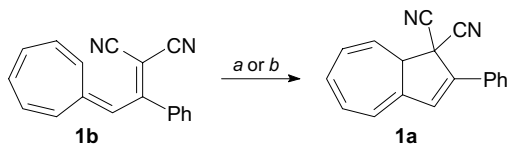
As an alternative to photoisomerization, Lewis acids like $AlCl_3$ and BBr_3 can promote ring-opening of DHA.[36] In particular, treatment of a solution of DHA (**1a**) in dichloromethane with $AlCl_3$ followed by water addition is a convenient way of obtaining VHF (**1b**) on a preparative scale in the absence of light (Scheme 3).[36]

Scheme 3



The VHF-to-DHA back-reaction was found to be promoted by $ZnCl_2$ or $Ag(OTf)\cdot(Et_2O)_3$ when conducted in dichloroethane – diethylether or 1,2-dichloroethane.[36] The strongest effect was, however, observed by using $Cu(MeCN)_4BF_4$;[37] addition of one equivalent of this Cu^I salt to VHF (**1b**) in dichloromethane reduced the half-life from 545 min to 18 – 22 min (Scheme 4). We assume that Cu^I coordinates to one of the cyano groups, and that this coordination promotes the VHF ring closure.

Scheme 4



(*a*) CH_2Cl_2: $t_{1/2}$ = 545 min;
(*b*) $Cu(MeCN)_4BF_4$ (1 equiv.), CH_2Cl_2: $t_{1/2}$ = 18 – 22 min

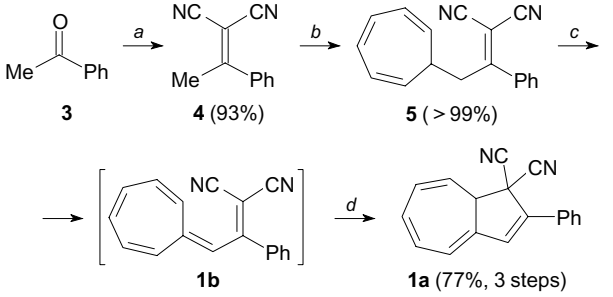
The copper-induced VHF-to-DHA transformation was successfully applied in a prototype photoconversion device.[35] Furthermore, the use of a demetallation agent as copper scavenger has shown that the efficiency of the DHA – VHF system was not compromized and recyclability is possible.[37]

6. Dihydroazulene synthesis

Synthetic strategies for obtaining DHA (**1a**) and its further functionalization were recently reviewed.[38] For this reason, here we shall cover only the synthesis employed most often (differing from the synthesis first reported by Daub *et al.*[18]) and a couple of functionalization methods. Further synthetic transformations will be shown when covering specific structures below.

Dihydroazulene (**1a**) is readily prepared on a multigram scale according to Scheme 5;[19] this protocol follows a route reported by Diederich and co-workers[39] for preparing the corresponding 4-iodophenyl-substituted DHA. The high-yielding protocol starts by the Knoevenagel condensation between acetophenone (**3**) and malononitrile, generating product **4**. Deprotonation of this compound and treatment with tropylium tetrafluoroborate gave product **5**, which was oxidized by hydride abstraction using tritylium tetrafluoroborate and subsequently deprotonated by triethylamine to generate the exocyclic fulvene bond and hence the vinylheptafulvene structure **1b**. This compound was then thermally converted, without isolation, to the final product **1a** (isolated as a racemic mixture of two enantiomers).

Scheme 5

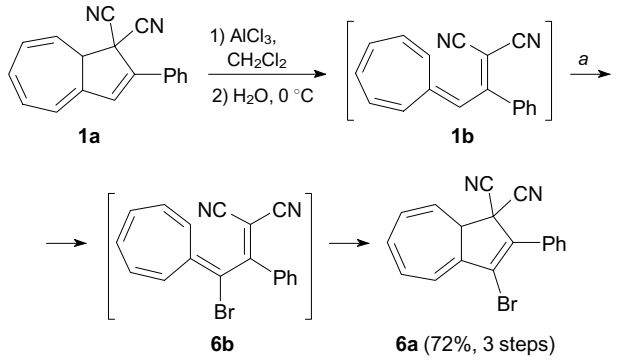


(*a*) NC⌒CN , AcOH, NH_4OAc, PhMe, reflux;
(*b*)  BF_4^-, Et_3N, CH_2Cl_2, −78 °C;
(*c*) 1) Ph_3CBF_4, $ClCH_2CH_2Cl$, 80 °C; 2) Et_3N, PhMe, 0 – 20 °C;
(*d*) $ClCH_2CH_2Cl$, PhMe, 80 °C

Two bromination protocols were developed for introducing a bromine atom at positions C(3) and C(7), respectively. The first functionalization is shown in Scheme 6. Dihydroazulene (**1a**) was converted to VHF (**1b**) using $AlCl_3$. The subsequent radical bromination with *N*-bromosuccinimide (NBS), benzoyl peroxide, and light furnished 3-bromo-substituted DHA **6a** *via* the intermediate VHF **6b**.[40]

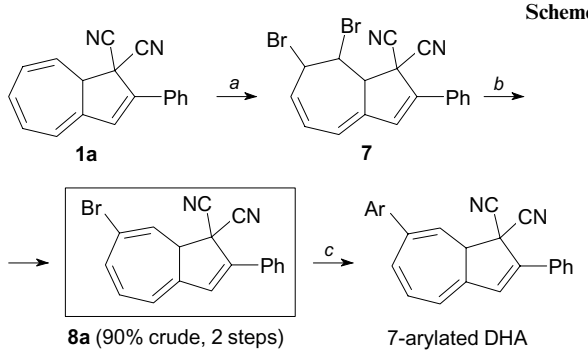
The regioselective bromination at position C(7) was accomplished according to Scheme 7.[41 – 43] First, DHA

Scheme 6

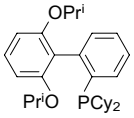


(*a*) NBS, $(PhCO_2)_2$, PhH, *hv*; NBS is N-bromosuccinimide

Scheme 7



(*a*) Br_2, CH_2Cl_2, −78 °C; (*b*) Li[Si(NMe$_2$)$_3$], THF, 0 °C;
(*c*) $ArB(OH)_2$, $Pd(OAc)_2$ (5 mol.%), RuPhos (10 mol.%),
K_3PO_4 (2 equiv.), PhMe – H_2O (9 : 1), r.t. several hours;
Ar = 4-RC_6H_4, R = CN, Me, Br, Bu^{t}S;

RuPhos =  (Cy is cyclohexyl)

(**1a**) was brominated by Br_2, and the resulting dibromide **7** was then treated with lithium hexamethyldisilazide (LiHMDS) to give the product **8a**. This product is rather unstable and is, in general, used crude for further reactions.

While 7-bromo-substituted DHA (**8a**) readily underwent Pd-catalyzed cross-coupling reactions such as Sonogashira and Suzuki couplings,[30, 31, 42, 43] allowing incorporation of various functional groups at position C(7) (see Scheme 7), it was rather challenging to use the 3-bromo-substituted analogue for such reactions; often fully unsaturated azulene products resulted instead.[33, 40] Suzuki arylation of **8a** under optimum conditions gave the arylation products in *ca.* 60% yields.

7. Computational screenings: towards high energy densities

Computational studies on how the energy density (Gibbs free energy gap between ground-state VHF and DHA isomers) of the system can be systematically tuned by functionalization have been conducted at the DFT level using M06-2X/6-311 + G(d).[25, 26] Another theoretical approach was moved forward by Saritas and Grossman,[44] but our recent theoretical investigations on energy storage capacity of the NBD – QC couple have shown that using the method M06-2X/6-311 + G(d) gives excellent agreement with experimental data,[45] and it is in our opinion the method of choice when calculating energy storage capacities.

We shall here discuss some of the most relevant theoretical results. Fig. 7 summarizes the effect on energy densities of structural modifications at different positions. The parent system **1a** – **1b** has an energy density of only 0.11 MJ kg^{-1} (see [25]). Placing a cyano group at C(7) (compound **9a**) does not compromise the energy density,[46] while it is an important modification for slowing the back-reaction (*vide infra*). Instead, by introducing an amino group at C(3) (compound **10a**), the energy density is doubled (0.22 MJ kg^{-1}).[26] A similar strong effect is

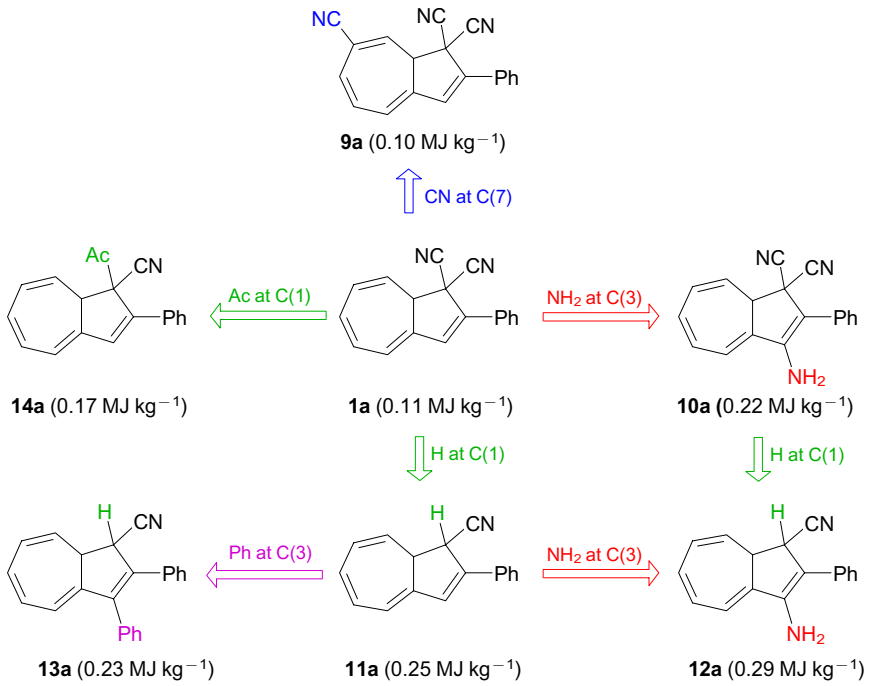
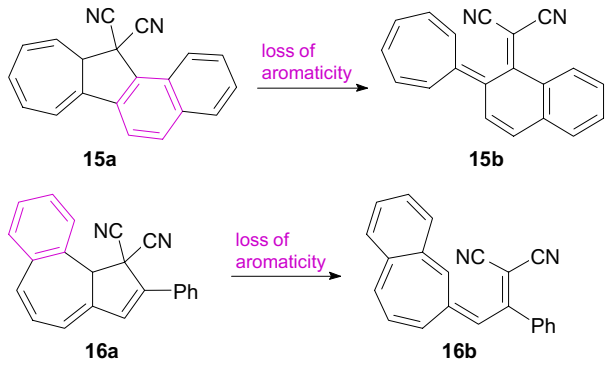


Figure 7. Calculated energy densities (difference in Gibbs free energy values between VHF and DHA isomers *in vacuo*; only DHA isomers are shown here) at the M06-2X/6-311 + G(d) level. For the specific diastereoisomers investigated for compounds **11a** – **14a**, we refer to the original literature.

achieved by replacing one cyano group with a hydrogen atom (**11a**), resulting in a density of 0.25 MJ kg^{-1} (see [47]). The combined effect of the last two modifications results in a density of 0.29 MJ kg^{-1} for compound **12a**.[26] Compound **11a** was found to be photoactive (*vide infra*), but the corresponding VHF would not return to DHA.[47] Other studies have shown that having a phenyl substituent at position C(3) of **1a** strongly enhances the back-reaction;[33, 48] while replacing the hydrogen atom at C(3) position of **11a** with a Ph group increases the molecular weight (generating compound **13a**), the energy density, gratifyingly, decreased only to 0.23 MJ kg^{-1}. With this modification, some degree of thermal isomerization of the corresponding VHF **13b** was in fact observed at elevated temperature, but it was, unfortunately, accompanied with decomposition.[47] Replacing one cyano group of **1a** with an acetyl group caused an increase in energy density (0.17 MJ kg^{-1} for compound **14a**),[49] but in this case, the corresponding VHF had a very short lifetime (*vide infra*).

To reach even higher energy densities, we introduced a new approach: loss(gain) of aromaticity during isomerization. Thus, we reasoned that if the DHA-to-VHF isomerization is accompanied by the loss of aromaticity of a benzenoid unit fused to the system as illustrated in Scheme 8, a larger energy difference should result. Indeed, calculations show that benzannulations at either positions C(2),C(3) (five-membered ring) or C(7),C(8) (seven-membered ring) result in energy densities of 0.38 MJ kg^{-1} (**15a**) and 0.28 MJ kg^{-1} (**16a**), respectively (Fig. 8).[50, 51] If, in addition, one cyano group of **15a** is replaced by a hydrogen atom (compound **17a**), an energy density of 0.51 MJ kg^{-1} is reached. The loss of aromaticity is not the sole reason for the higher energy density of **15b**. Thus, locking the DHA by an ethylene bridge between C(3) and phenyl on C(2) (**18a**)[52] affords a locked s-*cis* conformer of the corresponding VHF and a doubling of the energy density relative to the parent system.[50]

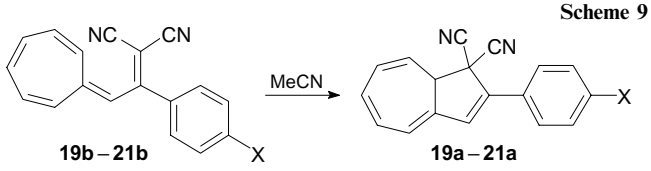
Scheme 8



8. Functionalization at position C(2)

A large selection of DHAs with EDGs or EWGs at position C(2) of the phenyl ring was prepared, and the rates of ring closure of the corresponding VHFs were determined experimentally.[31, 32, 42, 43] The syntheses relied on using functionalized acetophenones as starting materials, following a route similar to that outlined in Scheme 5, and when products contained a halide (Br or I) on the phenyl ring, further functionalization could be done by Pd-catalyzed reactions (such as cyanation). It was found that electron-donating groups decrease the rate of ring closure (in line with the TS structure shown in Figure 5), and when plotting ln k against Hammett substituent constants, a linear relationship was obtained.[32] Some of the longest half-lives ($t_{1/2}$, MeCN, 25 °C) were obtained for the VHFs **19b** – **21b** shown in Scheme 9.

Scheme 9



X = OMe (**19b**, $t_{1/2}$ = 230 min), Me (**20b**, $t_{1/2}$ = 255 min); NH_2 (**21b**, $t_{1/2}$ = 287 min)

Similarly, electron-withdrawing groups increased the rate of ring closure. The faster back-reaction when an EWG is present at C(2) stimulated the synthesis of DHA (**22a**) (Scheme 10).[53] This DHA contains a pyridyl group that can act as a site for protonation (deprotonation); acid (base) stimuli could thereby be employed to spark (halt) energy release. Dihydroazulene (**22a**) exhibits an absorption

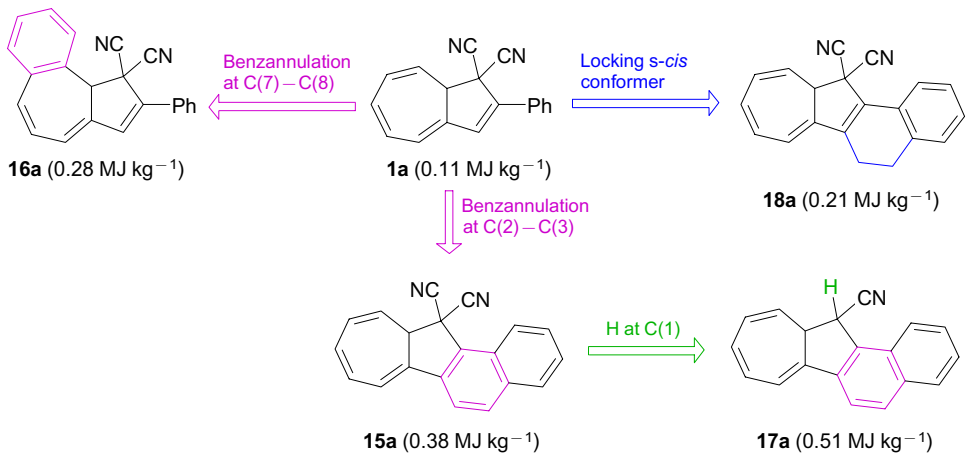
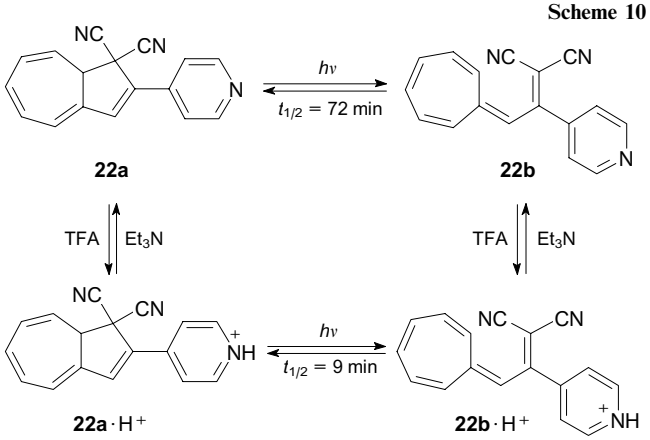


Figure 8. Calculated energy densities (difference in the Gibbs free energy values between VHF and DHA) at the M06-2X/6-311 + G(d) level.

Scheme 10

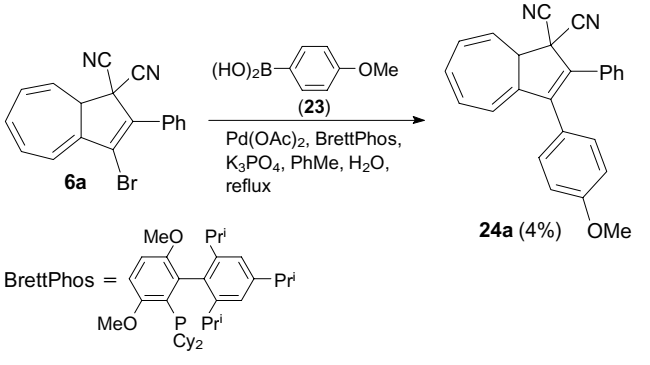


maximum at 359 nm and photoisomerizes into VHF (**22b**) showing an absorption maximum at 480 nm. This VHF had a half-life of 72 min (MeCN, 25 °C). Yet, protonation of the pyridine ring by trifluoroacetic acid (TFA) promotes the back-reaction due to the stronger electron-withdrawing character of the protonated substituent, and a half-life of only 9 min was obtained for **22b** · H^+. The protonated DHA species (**22a** · H^+) exhibited a significantly red-shifted absorption maximum (406 nm) relative to that of the neutral DHA **22a** (359 nm). Acid has also been employed for stimulating the thermal back-reaction of other systems; *e.g.*, the cycloreversion of a diarylethene.[17]

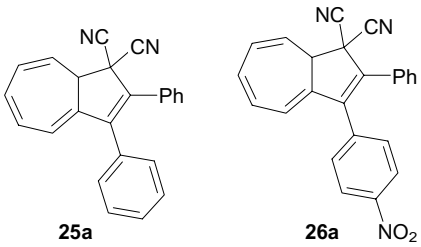
9. Functionalization at position C(3)

3-Bromo-substituted DHA (**6a**) was not particularly reactive for Suzuki coupling reactions.[33,40] It was possible, however, to introduce a *p*-methoxyphenyl substituent at this position by coupling with the boronic acid (**23**), providing DHA (**24a**), albeit in low yield (Scheme 11).[33] 3-Phenyl and 3-(4-nitrophenyl) substituted derivatives **25a** and **26a** were instead prepared by following a protocol similar to the one outlined in Scheme 5 with the aryl group incorporated already onto the acetophenone starting material. The resulting VHFs underwent extremely fast back-reactions, which were therefore followed at −20 °C in EtOH. Half-lives of 20 min (**24b**; OMe substituent on phenyl), 25 min (**25b**; no substituent), and 43 min (**26b**; NO_2 substituent) were obtained. A Hammett correlation was established when plotting $\ln k$ against σ_p, but the correlation was only based on these three data points.

Scheme 11



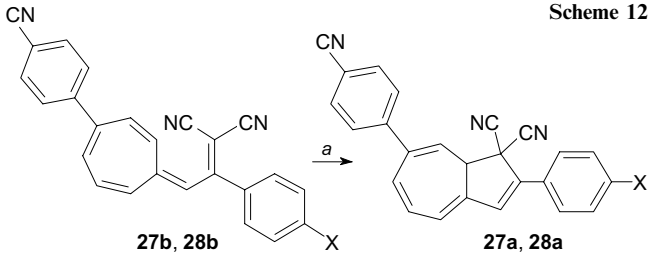
Structures 25a, 26a



10. Functionalization at position C(7)

Employing the bromination – elimination protocol described in Section 7 followed by the Suzuki arylation furnished a large selection of arylated DHAs substituted with C_6H_4X at position C(7) (with X being EDG or EWG).[31,43] As in the case for the C(2) functionalization, a Hammett correlation for VHF-to-DHA ring closure was obtained for these compounds,[32] but with the opposite influence of the electron-donating (withdrawing) character of the substituent. Thus, now introduction of EWGs enhanced the VHF lifetime, and compound **27b** (Scheme 12) exhibited the longest half-life (641 min, MeCN, 25 °C). By introducing a CN acceptor group at C(7) and Me donor group at C(2) [VHF (**28b**)], the half-life was extended to 668 min.

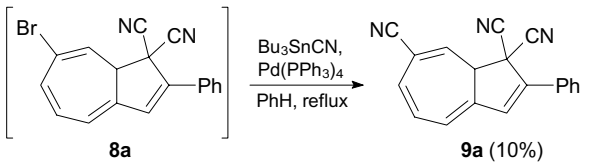
Scheme 12



(*a*) MeCN;
X = H (**27**), Me (**28**)

To achieve a more effective influence, acceptor groups were recently incorporated directly at position C(7) without an intermediate benzene ring.[46] For example, introduction of CN was accomplished according to Scheme 13. The bromo-functionalized intermediate **8a**, prepared crude by bromination of DHA (**1a**) followed by elimination of HBr according to Scheme 7, was treated with Bu_3SnCN and $Pd(PPh_3)_4$, which gave product **9a**. The yield was rather low, but alternative procedures have so far not been reliable. The absorption maximum of **9a** (360 nm) is not significantly altered relative to that of **1a**. Instead, the functionalization has a significant influence on the lifetime of the corresponding VHF. Thus, photoisomerization of **9a** provided VHF **9b** (*E*/*Z* isomers) having a half-life of 1.3×10^3 min (MeCN, 25 °C). As a result, the half-life is doubled relative to that of **27b**. At the same time, the functionalization does not compromise energy density to any significant degree (see Fig. 7). For comparison, also for the norbornadiene – quadricyclane couple the direct linkage of a cyano group to one of the sp^2-hybridized carbon atoms rather than linkage of the larger *p*-cyanophenyl acceptor group has been reported as an advantage in the context of MOST systems.[54]

Scheme 13



8a **9a** (10%)

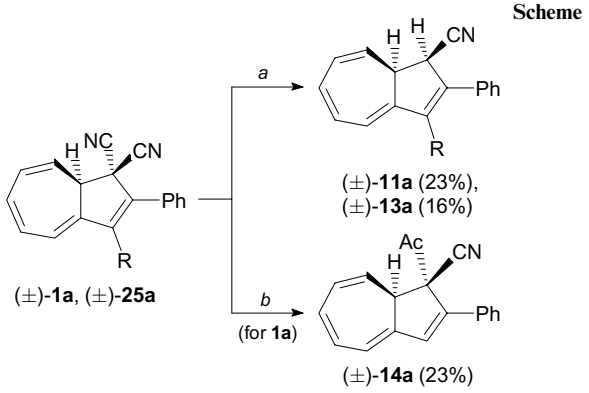
11. Replacing one cyano group at position C(1)

Changing the substituent groups at position C(1) had the strongest influence on the energy density as described above. Moreover, the character of the substituent groups at this position has a huge influence on the VHF lifetime (relating to whether or not these can stabilize negative charge at this carbon atom, *cf.* TS structure shown in Figure 5). In terms of synthesis, the simplest approach has proven to be the direct modification of one cyano group on the preformed, parent DHA (**1a**). The introduction of a group other than cyano at position C(1) induces the formation of a mixture of four possible stereoisomers as two enantiomeric pairs. Independently from the specific reaction, a higher reactivity of the nitrile opposite to the seven-membered ring has been detected, producing a major diastereoisomer.

Treatment of DHAs **1a** and **25a** with DIBAL-H resulted in each case in the replacement of one cyano group by a hydrogen atom, furnishing products **11a** and **13a**, respectively (Scheme 14, conditions *a*; only the major diastereoisomer is shown in each case).[47] For **11a**, only the major diastereoisomer was isolated (as an enantiomeric pair), while for **13a** both were isolated (again as enantiomeric pairs) in a 6 : 1 ratio; the structure of the major isomer was confirmed by X-ray crystallography. The longest-wavelength absorption maximum of **11a** is at 353 nm in MeCN, *i.e.*, similar to that of **1a**. Upon irradiation at 353 nm, a full conversion into the corresponding VHF was achieved. This compound has a characteristic absorption maximum at 379 nm, hence, it is significantly blue-shifted relative to VHF (**1b**). The VHF (**11b**) was, however, unable to thermally revert to DHA, not even at elevated temperature. Compound **13a** was photoactive like **11a** and could be photoisomerized. Partial back-conversion of the VHF into DHA was observed upon heating (70 °C, MeCN, 72 h), but the conversion was accompanied by degradation. From transition state calculations, a half-life of >10 years at ambient temperature and 160 h at 70 °C was obtained for VHF (**13b**). Decomposition of these systems limits their use, but the results show that it is indeed possible to enhance both the energy density and the VHF lifetime by one structural modification. Yet, not all modifications at position C(1) met this attractive feature. Upon replacement of the hydrogen atom with an acetyl group (compound **14a**), the energy density is still increased relative to the parent system (see Figure 7).[49] This functionalization, however, compromises the VHF lifetime, being very short. Synthetically, DHA **14a** was accomplished by treating **1a** with lithium naphthalenide (LN) in THF followed by quenching with acetyl chloride (Scheme 14, conditions *b*); the product was isolated as a single diastereoisomer (as a racemic mixture). After irradiation of this diastereoisomer with light in acetonitrile, no VHF form was detected, neither by means of UV-Vis absorption spectroscopy nor by NMR spectroscopy. Instead, a mixture of DHA diastereoisomers was found, suggesting that a very fast VHF-to-DHA back-reaction occurred. In a more apolar solvent (cyclohexane) it was in fact possible to detect VHF (**14b**) and determine its half-life of only a few minutes at 25 °C.

The faster ring closure reaction of the VHF acetyl derivative **14b** and the extremely slower ring closure reaction of its decyanated analogue **11b** in comparison with the parent system **1b** indicates that the influence of a C(1)-substituent is difficult to rationalize just in terms of electronic character of the functional groups. Nevertheless, for the series of compounds **29a** – **32a** having a common benzothiazole group at C(1), an influence of the electronic character of the substituent group at the benzothiazole benzene ring was observed.[34] First, VHFs of these compounds underwent ring closure much faster than the parent

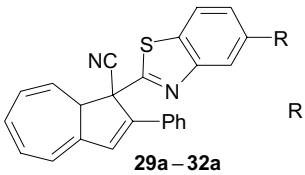
Scheme 14



(±)-**1a**, (±)-**25a** (±)-**14a** (23%)

(*a*) DIBAL-H, THF, 0 °C;
(*b*) 1) LN, −78 °C, 2) AcCl, THF, −78 °C to rt;
R = H (**1a**, **11a**), Ph (**13a**, **25a**); DIBAL-H = $(Bu^i_2AlH)_2$;
LN is lithium naphthalenide

Structures 29a – 32a



29a – 32a

R = H (**29a**), Cl (**30a**),
CF_3 (**31a**), OMe (**32a**)

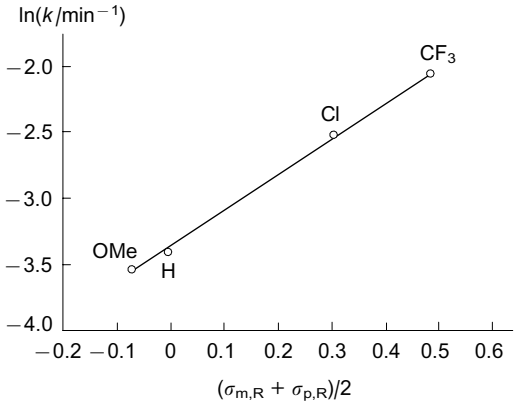


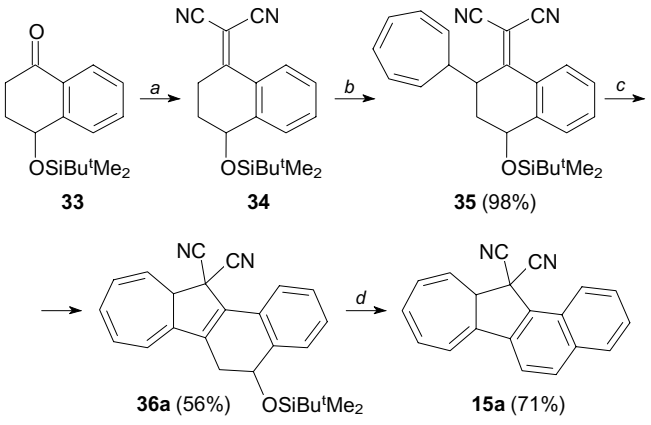
Figure 9. Hammett correlation for ring closure of VHFs generated from DHAs **29a** – **32a**. Rate constants (k) were determined at 5 °C in MeCN. $\sigma_{p,R}$ and $\sigma_{m,R}$ are the Hammett substituent constants for *para*- and *meta*-substituents R.[34]

VHF (**1b**), and experiments therefore had to be conducted at 5 °C in MeCN. At this temperature, a Hammett correlation was obtained when plotting $\ln k$ against the average of Hammett substituent constants, for *meta*- and *para*-substituents ($\sigma_{p,R}$ and $\sigma_{m,R}$) (Fig. 9). In this series of compounds, an electron-withdrawing substituent (CF_3 or Cl) accelerates the ring closure reaction.

12. Benzannulation of the five-membered ring

Benzannulation of the five-membered ring was accomplished according to Scheme 15.[50] First, ketone **33** was converted into the Knoevenagel product **34** by treatment with malononitrile using an AcOH – HMDS buffer. This compound was then treated with tropylium tetrafluoroborate in the presence of Et_3N to give **35**, which was subjected to two-step oxidation using $NOBF_4$ followed by pyridine to be converted to the VHF that immediately underwent a ring-closure to form DHA (**36a**). Finally, a desilylation – elimination reaction upon treatment with TsOH in refluxing benzene gave product **15a**.

Scheme 15



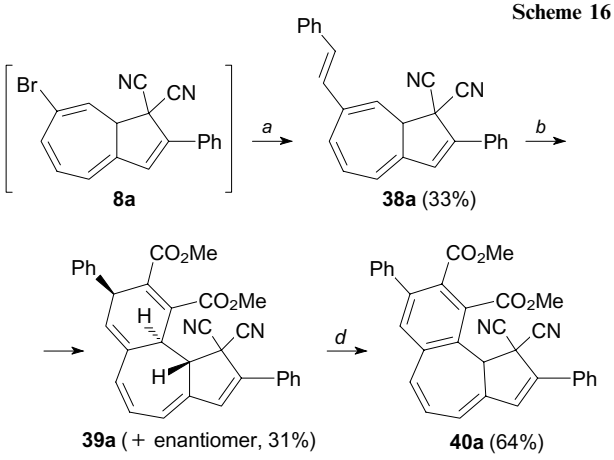
(*a*) NC–⟨⟩–CN, $NH(SiMe_3)_2$, AcOH, reflux;
(*b*) ⟨⟩$^+$ BF_4^-, Et_3N, CH_2Cl_2, −78 °C;
(*c*) 1) $NOBF_4$, MeCN, −40 °C; 2) Py, CH_2Cl_2, −40 °C;
(*d*) TsOH·H_2O, PhH, reflux

Dihydroazulene **15a** exhibited a characteristic absorption at λ_{max} = 342 nm in EtOH and cyclohexane. Irradiation at 365 nm did not provide the desired VHF **15b**; instead, other photolysis products were formed. Yet, it was possible to chemically convert **15a** into **15b** by treatment with either BBr_3 or $AlCl_3$ to form a complex. The addition of water broke up the complex and the VHF was found to instantaneously return to DHA. Thus, benzannulation at positions C(2), C(3) has compromised the desired switching properties. The fast back-reaction of VHF **15b** may to some extent arise from locking it in the reactive s-*cis* conformation. Indeed, DHA **18a** (see Fig. 8) was found to be photoactive, undergoing conversion to a VHF form, which returned within milliseconds to DHA in EtOH.[52]

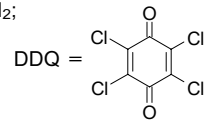
13. Benzannulation of the seven-membered ring

Fusing instead a benzene ring to the seven-membered ring would prevent fixing the VHF in its reactive s-*cis* conformation. Therefore, a derivative of compound **16a** was prepared (Scheme 16).[51] 7-Bromo-DHA **8a** was reacted with the boronic acid **37** under Suzuki cross-coupling conditions to furnish the styrene-substituted DHA **38a**. The reaction of **38a** with dimethyl acetylenedicarboxylate under microwave (MW) heating gave the Diels – Alder cycloadduct **39a**. A final oxidation using 2,3,-dichloro-5,6-dicyano-1,4-benzoquinone (DDQ) gave the benzo-fused product **40a**.

Scheme 16



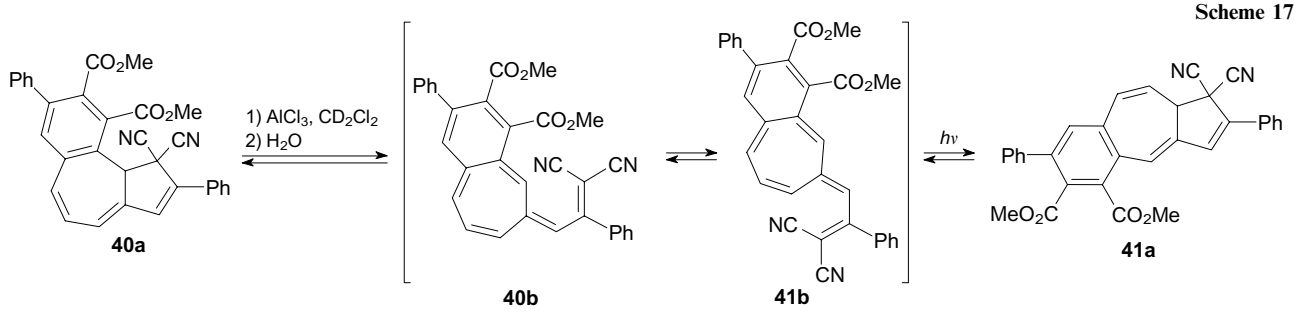
(*a*) Ph–⟨⟩–B(OH)$_2$ (**37**), $Pd(OAc)_2$, K_3PO_4, RuPhos, PhMe, H_2O;
(b) MeO_2C–≡–CO_2Me, PhMe, 140 °C (MW);
(*c*) DDQ, CH_2Cl_2;



The benzo-fused DHA **40a** has a longest-wavelength absorption maximum (354 nm in cyclohexane, 355 nm in acetone, 358 nm in EtOH) close to that of the parent system **1a**. Interestingly, in contrast to the latter compound, benzo-fused DHA **40a** is, however, strongly fluorescent. Upon irradiation, the desired VHF was not formed. Instead, treating the DHA with $AlCl_3$ and then by water promoted the formation of the corresponding VHF, but it could not be isolated as it underwent the fast ring-closure. The UV-Vis absorption spectrum of the product was not identical to that of **40a**. Thus, the characteristic DHA absorption was slightly blue-shifted [from 358 to 352 nm (EtOH)] and significantly more intense. ^{1}H-NMR spectroscopic analysis as well as X-ray study revealed a transformation into isomeric DHA (**41a**). This isomerization likely results from a conversion between VHFs **40b** (*Z*-isomer) and **41b** (*E*-isomer) before the ring-closure occurs (Scheme 17).

The blue-shifted absorption of **41a** was somewhat surprising, but absorption spectra calculated using CAM-B3LYP/6-311 + G(d,p) showed the exact same trend (Fig. 10). Gratifyingly, DHA **41a** was found to be photoactive, but the formed VHF quickly returned to either **41a** or **40a**. Thus, ultimately all material would become trapped as the non-photoactive DHA **40a**. The difference in photoactivity between DHA isomers **40a** and **41a** was explained in a theoretical study performed on the corresponding unsubstituted compounds (**16a** and **42a**) by considering changes in anti-aromaticity on the excited state surface as illustrated schematically in Fig. 11.[55] In the case of compound **42a**, excitation leads to an anti-aromatic structure as well as an

Scheme 17



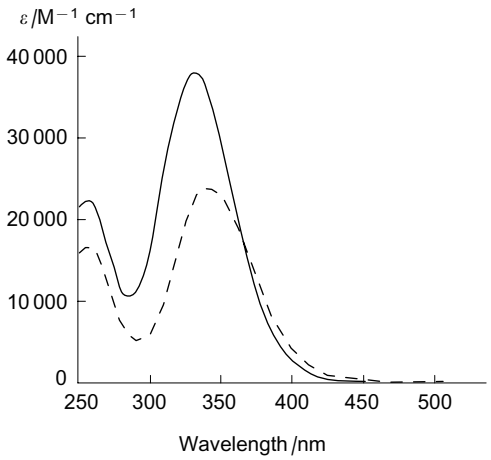


Figure 10. Calculated UV-Vis absorption spectra of compound **40a** (dashed line) and **41a** (solid line) in EtOH using CAM-B3LYP/6-311+G(d,p) and the IEF-PCM solvation model.[51] ε is molar absorptivity.

anti-aromatic TS towards VHF (**42b**). Excitation of **16a** leads instead to a non-aromatic structure that has to pass an unfavourable anti-aromatic TS towards VHF (**16b**).

14. Macrocyclic structures

Introduction of photoswitching units into macrocycles can significantly alter isomer stabilities and switching capabilities as recently reviewed.[56] The DHA dimer **43** (a mixture of diastereoisomers)[57] was incorporated in macrocyclic structures of different ring sizes according to Scheme 18.[58, 59] The bromine atom was introduced into both DHAs by the regioselective bromination – elimination protocol, forming first intermediate **44** and then DHA dimer **45**, which was next subjected to two Suzuki coupling reactions with the benzylic alcohol **46**. Finally, macrocyclization reactions were performed by treating the obtained diol **47** with acid chlorides of various lengths, furnishing macrocycles **48** – **50** as a mixture of diastereoisomers that could be separated.

All three macrocycles were photoactive in sequential ring-opening reactions ultimately forming the VHF-VHF macrocycles (Scheme 19). Some slight differences in the

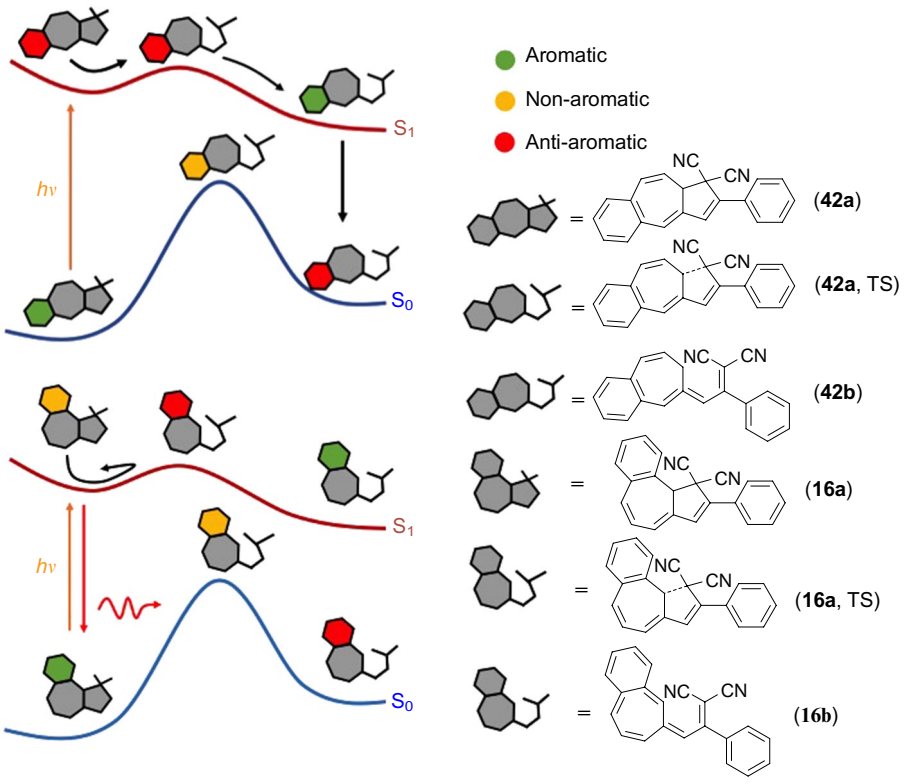
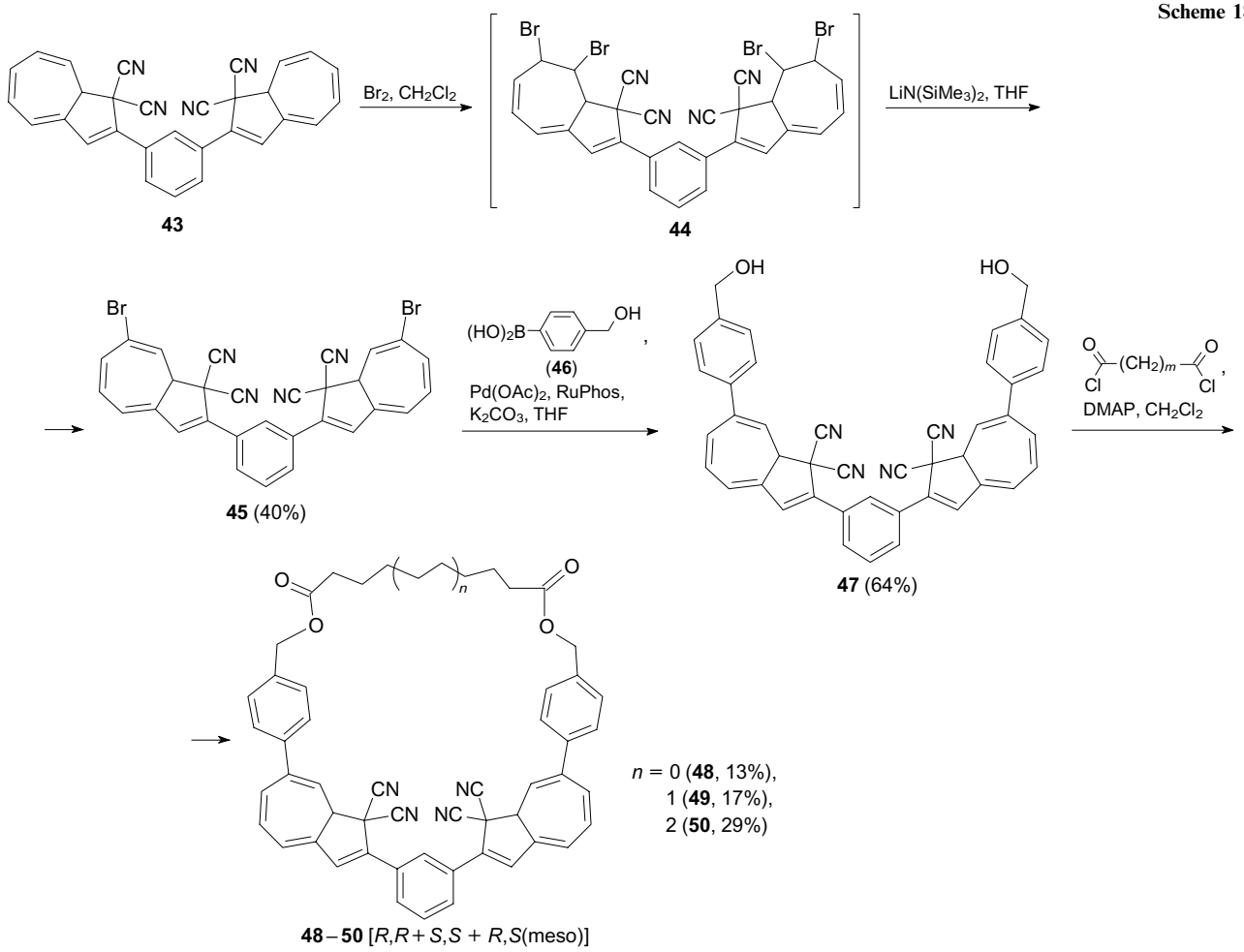


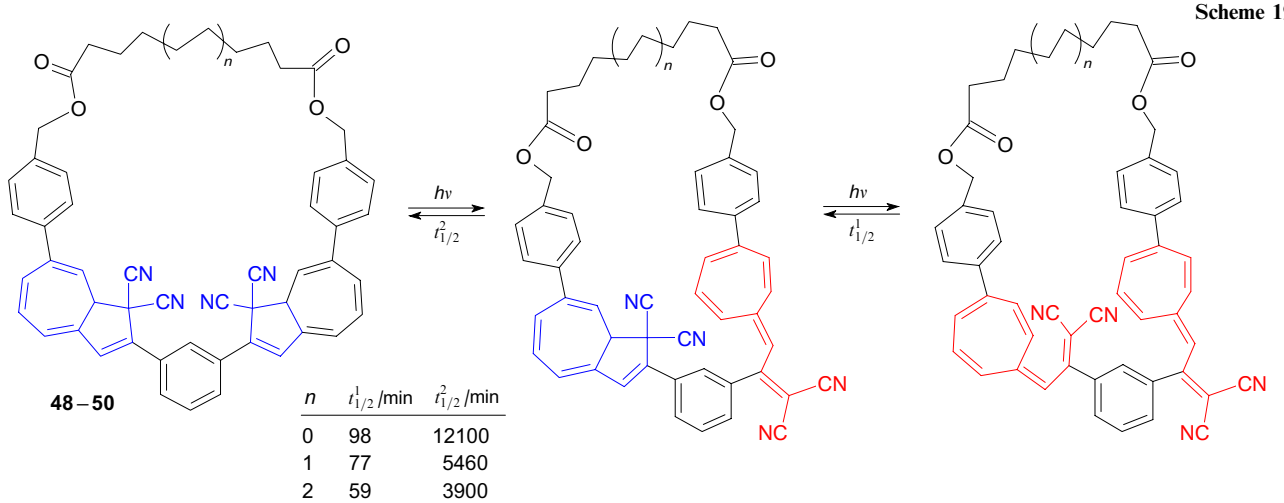
Figure 11. Schematic illustration of the aromaticity changes on the ground (S_0) and excited (S_1) singlet state energy surfaces during benzo-fused DHA-to-VHF interconversions.[55]

Scheme 18



ring-opening reactions have been recorded, but the common trend is that the first DHA unit underwent a ring-opening at a similar rate as the parent DHA, while the second DHA unit opened at least 30 times slower. The resulting VHF-VHF macrocycles were also found to undergo stepwise ring-closures. The stepwise ring closure can be beneficial for MOST systems, which can take profit of energy release on different time scales. The half-lives of these ring-closure reactions increased with decreasing ring size (see Scheme 19). Notably, the second ring-closure reaction has a half-life that increases from 3900 min to 12100 min (MeCN, 25 °C) when proceeding from **50** to **48**. As observed for the parent VHF, the ring closure can be promoted by Cu(I) ions. For the VHF-VHF macrocycle of **49** (n = 1), an overall discharge of 10% was measured in acetone at 25 °C within 24 h, while in the presence of Cu^{I} (> 2 equiv. per DHA unit), a 10% discharge was achieved within only 2 – 3 h.[37] In CH_2Cl_2, addition of Cu^{I} (> 2 equiv. per DHA unit) resulted in VHF half-lives of only 69 and 534 min.

Scheme 19

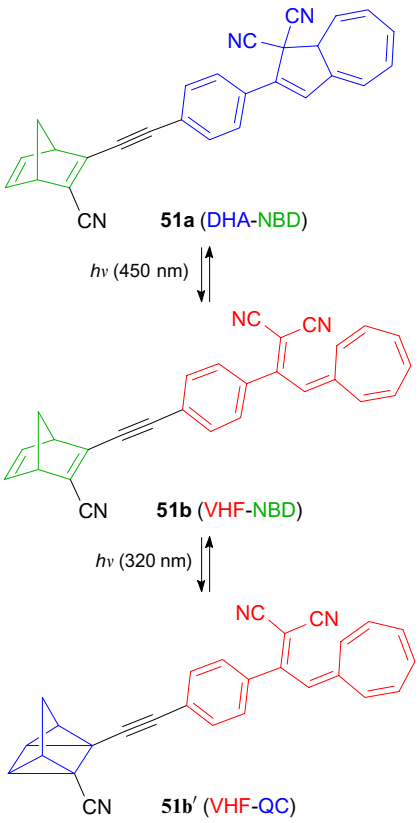


n	$t^1_{1/2}$ /min	$t^2_{1/2}$ /min
0	98	12100
1	77	5460
2	59	3900

15. Dihydroazulene — norbornadiene conjugates

The DHA photoswitch has also been combined with other photoswitches aiming at enhancing the energy density as well as tuning the absorption maxima towards longer wavelengths. One such example is provided by the DHA–NBD conjugate (**51a**) shown in Scheme 20.[60] The parent, unsubstituted NBD–QC couple is particularly attractive for its large energy density (1 MJ kg^{-1}),[8] while it only absorbs in the UV region. The conjugate **51a** has an absorption maximum at 392 nm ($\varepsilon = 34.1 \times 10^3$ M^{-1} cm^{-1}), significantly red-shifted relative to that of DHA (**1a**). The DHA and NBD units could be photoisomerized in a stepwise matter into VHF (forming **51b**) and QC (forming **51b′**) units by first irradiating with 450-nm light and thereafter with 320-nm light, while it was not possible to convert NBD before DHA by using lower-wavelength light (290 nm). The QC and VHF units returned to the original NBD and DHA units with half-lives estimated as 11 and 70 min (PhMe, 50 °C), respectively. Calculations reveal an energy density of 0.27 MJ kg^{-1} in toluene for the VHF–QC isomer **51b′**.

Scheme 20



16. Conclusion

We have summarized the multiple ways available to tune the switching ability, energy density, and absorption properties of the DHA-VHF system, that is, by i) functionalizations at various positions of the core, ii) benzannulations, iii) macrocyclizations, iv) combination with other photoswitches, and v) metal ion catalysis or acid (base) stimuli (triggering energy release). Some of the structural variations work together in regard to optimizing some properties for solar energy storage, while others counteract and, in some cases, compromise the switching character of the system.

We believe that there is still plenty of room for combining the extensive structure–property relationships collected in the last decade on DHA derivatives and finding one optimum DHA-based molecule for MOST applications. Carefully combined hybrid photoswitches, constituted by a suitably functionalized DHA and other photoswitches, seem, in our opinion, to be a particularly attractive approach for future development. Specific advantages of each photoswitch could indeed work in concert to reach broader absorption profiles, higher energy densities, and energy releases on timescales that can ultimately be altered by suitable catalysts. One approach to higher energy densities could also be cascade-like systems where one photoisomerization event leads to structural changes of the molecule that generates a new photoswitch unit, which absorbs a second photon and generates, upon photoisomerization, a third photoswitch unit, *etc*., in this way keeping the molecular weight low as structural units of a generated photoisomer become part of the new photoswitch unit being formed. One such approach has been described theoretically for photoisomerization of a DHA into a VHF where its vinyl double bond is the central ethene unit of a dithienylethene photoswitch,[27] but this system still has to be synthesized and studied experimentally.

Figure 2 is reprinted with permission from PCCP Owner Societies, Fig. 3 is reprinted with permission from American Chemical Society, Fig. 6, 9, 10 and 11 are reprinted with permission from Wiley.

References

1. IPCC, 2014: Summary for Policymakers. In *Climate Change 2014: Mitigation of Climate Change. Contribution of Working Group III to the Fifth Assessment Report of the Intergovernmental Panel on Climate Change*. (Eds O.Edenhofer, R.Pichs-Madruga, Y.Sokona, E.Farahani, S.Kadner, K.Seyboth, A.Adler, I.Baum, S.Brunner, P.Eickemeier, B.Kriemann, J.Savolainen, S.Schlömer, C.von Stechow, T.Zwickel, J.C.Minx). Cambridge University Press, Cambridge, United Kingdom and New York, NY, USA. https://www.ipcc.ch/site/assets/uploads/2018/03/WGIIIAR5_SPM_TS_Volume-3.pdf (accessed 2019-09-19)
2. IPCC, 2018: Summary for Policymakers. In *Global Warming of 1.5 °C. An IPCC Special Report on the Impacts of Global Warming of 1.5 °C above Pre-industrial Levels and Related Global Greenhouse Gas Emission Pathways, in the Context of Strengthening the Global Response to the Threat of Climate Change, Sustainable Development, and Efforts to Eradicate Poverty*. (Eds V.Masson-Delmotte, P.Zhai, H.-O.Pörtner, D.Roberts, J.Skea, P.R.Shukla, A.Pirani, W.Moufouma-Okia, C.Péan, R.Pidcock, S.Connors, J.B.R.Matthews, Y.Chen, X.Zhou, M.I.Gomis, E.Lonnoy, T.Maycock, M.Tignor, T.Waterfield). World Meteorological Organization, Geneva, Switzerland. P. 32. https://www.ipcc.ch/site/assets/uploads/sites/2/2019/05/SR15_SPM_version_report_LR.pdf (accessed 2020-02-11)
3. IPCC, 2019: Summary for Policymakers. In *IPCC Special Report on the Ocean and Cryosphere in a Changing Climate*. (Eds H.-O.Pörtner, D.C.Roberts, V.Masson-Delmotte, P.Zhai, M.Tignor, E.Poloczanska, K.Mintenbeck, M.Nicolai, A.Okem, J.Petzold, B.Rama, N.Weyer). P. 42. https://report.ipcc.ch/srocc/pdf/SROCC_FinalDraft_FullReport.pdf (accessed 2020-02-11)
4. E.Gimon, M.O'Boyle, C.T.M.Clack, S.McKee. *The Coal Cost Crossover: Economic Viability of Existing Coal Compared to New Local Wind and Solar Resources*. Vibrant Clean Energy, Energy Innovation, Mar 2019

5. J.Rugolo, M.J.Aziz. *Energy Environ. Sci.*, **5**, 7151 (2012)
6. P.Duffy, C.Fitzpatrick, T.Conway, R.P.Lynch. In *Issues in Environmental Science and Technology*. Royal Society of Chemistry, 2018. P. 1
7. REN21, 'Renewables 2019: Global status report'. REN21 Secretariat, Paris, http://www.ren21.net/gsr-2019/(accessed 20-04-2020)
8. Z.-i.Yoshida. *J. Photochem.*, **29**, 27 (1985)
9. A.D.Dubonosov, V.A.Bren, V.A.Chernoivanov. *Russ. Chem. Rev.*, **71**, 917 (2002)
10. Y.Kanai, V.Srinivasan, S.K.Meier, K.P.C.Vollhardt, J.C.Grossman. *Angew. Chem., Int. Ed.*, **49**, 8926 (2010)
11. T.J.Kucharski, Y.Tian, S.Akbulatov, R.Boulatov. *Energy Environ. Sci.*, **4**, 4449 (2011)
12. K.Moth-Poulsen. In *Organic Synthesis and Molecular Engineering*. (Ed. M.B.Nielsen). Wiley, USA, 2014. P. 179
13. A.Lennartson, A.Roffey, K.Moth-Poulsen. *Tetrahedron Lett.*, **56**, 1457 (2015)
14. L.Dong, Y.Feng, L.Wang, W.Feng. *Chem. Soc. Rev.*, **47**, 7339 (2018)
15. K.Edel, X.Yang, J.S.A.Ishibashi, A.N.Lamm, C.Maichle-Mössmer, Z.X.Giustra, S.-Y.Liu, H.F.Bettinger. *Angew. Chem., Int. Ed.*, **57**, 5296 (2018)
16. C.-L.Sun, C.Wang, R.Boulatov. *ChemPhotoChem*, **3**, 268 (2019)
17. J.Gurke, M.Quick, N.P.Ernsting, S.Hecht. *Chem. Commun.*, **53**, 2150 (2017)
18. J.Daub, T.Knöchel, A.Mannschreck. *Angew. Chem., Int. Ed. Engl.*, **23**, 960 (1984)
19. S.L.Broman, S.L.Brand, C.R.Parker, M.Å.Petersen, C.G.Tortzen, A.Kadziola, K.Kilså, M.B.Nielsen. *Arkivoc*, **ix**, 51 (2011)
20. S.L.Broman, M.B.Nielsen. *Phys. Chem. Chem. Phys.*, **16**, 21172 (2014)
21. H.Görner, C.Fischer, J.Daub. *J. Photochem. Photobiol. A Chem.*, **85**, 217 (1995)
22. M.Abedi, M.Pápai, K.V.Mikkelsen, N.E.Henriksen, K.B.Møller. *J. Phys. Chem. Lett.*, **10**, 3944 (2019)
23. O.Schalk, S.L.Broman, M.Å.Petersen, D.V.Khakhulin, R.Y.Brogaard, M.B.Nielsen, A.E.Boguslavkiy, A.Stolow, T.I.Sølling. *J. Phys. Chem. A*, **117**, 3340 (2013)
24. H.Görner, C.Fischer, S.Gierisch, J.Daub *J. Phys. Chem.*, **97**, 4110 (1993)
25. S.T.Olsen, J.Elm, F.E.Storm, A.N.Gejl, A.S.Hansen, M.H.Hansen, J.R.Nikolajsen, M.B.Nielsen, H.G.Kjaergaard, K.V.Mikkelsen. *J. Phys. Chem. A*, **119**, 896 (2015)
26. M.H.Hansen, J.Elm, S.T.Olsen, A.N.Gejl, F.E.Storm, B.N.Frandsen, A.B.Skov, M.B.Nielsen, H.G. Kjaergaard, K.V.Mikkelsen. *J. Phys. Chem. A*, **120**, 9782 (2016)
27. A.S.Gertsen, S.T.Olsen, S.L.Broman, M.B.Nielsen, K.V.Mikkelsen. *J. Phys. Chem. C*, **121**, 195 (2017)
28. N.Ree, M.H.Hansen, A.S.Gertsen, K.V.Mikkelsen. *J. Phys. Chem. A*, **121**, 8856 (2017)
29. B.N.Frandsen, A.B.Skov, M.Cacciarini, M.B.Nielsen, H.G.Kjaergaard. *Chem. – Asian J.*, **14**, 1111 (2019)
30. S.L.Broman, M.Å.Petersen, C.Tortzen, A.Kadziola, K.Kilså, M.B.Nielsen. *J. Am. Chem. Soc.*, **132**, 9165 (2010)
31. M.Å.Petersen, S.L.Broman, K.Kilså, A.Kadziola, M.B.Nielsen. *Eur. J. Org. Chem.*, 1033 (2011)
32. S.L.Broman, M.Jevric, M.B.Nielsen. *Chem. – Eur. J.*, **19**, 9542 (2013)
33. M.D.Kilde, M.H.Hansen, S.L.Broman, K.V.Mikkelsen, M.B.Nielsen. *Eur. J. Org. Chem.*, 1052 (2017)
34. D.Andersen, M.D.Kilde, A.Kadziola, M.Cacciarini, M.B.Nielsen. *Helv. Chim. Acta*, **101**, e1800153 (2018)
35. Z.Wang, J.Udmark, K.Börjesson, R.Rodrigues, M.Abrahamsson, M.B.Nielsen, K.Moth-Poulsen. *ChemSusChem*, **10**, 3049 (2017)
36. C.R.Parker, C.G.Tortzen, S.L.Broman, M.Schau-Magnussen, K.Kilså, M.B.Nielsen. *Chem. Commun.*, **47**, 6102 (2011)
37. M.Cacciarini, A.Vlasceanu, M.Jevric, M.B.Nielsen. *Chem. Commun.*, **53**, 5874 (2017)
38. M.Cacciarini, S.L.Broman, M.B.Nielsen. *Arkivoc*, **i**, 249 (2014)
39. L.Gobbi, P.Seiler, F.Diederich. *Helv. Chim. Acta*, **84**, 743 (2001)
40. V.Mazzanti, M.Cacciarini, S.L.Broman, C.R.Parker, M.Schau-Magnussen, A.D.Bond, M.B.Nielsen. *Beilstein J. Org. Chem.*, **8**, 958 (2012)
41. M.Å.Petersen, K.Kilså, A.Kadziola, M.B.Nielsen. *Eur. J. Org. Chem.*, 1415 (2007)
42. M.Jevric, S.L.Broman, M.B.Nielsen. *J. Org. Chem.*, **78**, 4348 (2013)
43. S.L.Broman, M.Jevric, A.D.Bond, M.B.Nielsen. *J. Org. Chem.*, **79**, 41 (2014)
44. K.Saritas, J.C.Grossman. *J. Phys. Chem. C*, **121**, 26677 (2017)
45. N.Ree, K.V.Mikkelsen. Unpublished results
46. J.Mogensen, O.Christensen, M.D.Kilde, M.Abildgaard, L.Metz, A.Kadziola, M.Jevric, K.V.Mikkelsen, M.B.Nielsen. *Eur. J. Org. Chem.* 1986 (2019)
47. M.Cacciarini, A.B.Skov, M.Jevric, A.S.Hansen, J.Elm, H.G.Kjaergaard, K.V.Mikkelsen, M.B.Nielsen. *Chem. – Eur. J.*, **21**, 7454 (2015)
48. T.Mrozek, H.Görner, J.Daub. *Chem. – Eur. J.*, **7**, 1028 (2001)
49. M.Cacciarini, M.Jevric, J.Elm, A.U. Petersen, K.V.Mikkelsen, M.B.Nielsen. *RSC Adv.*, **6**, 49003 (2016)
50. A.B.Skov, S.L.Broman, A.S.Gertsen, J.Elm, M.Jevric, M.Cacciarini, A.Kadziola, K.V.Mikkelsen, M.B.Nielsen. *Chem. – Eur. J.*, **22**, 14567 (2016)
51. A.B.Skov, J.F.Petersen, J.Elm, B.N.Frandsen, M.Santella, M.D.Kilde, H.G.Kjaergaard, K.V.Mikkelsen, M.B.Nielsen. *ChemPhotoChem*, **1**, 206 (2017)
52. S.L.Broman, O.Kushnir, M.Rosenberg, A.Kadziola, J.Daub, M.B.Nielsen. *Eur. J. Org. Chem.* 4119 (2015)
53. M.D.Kilde, P.G.Arroyo, A.S.Gertsen, K.V.Mikkelsen, M.B.Nielsen. *RSC Adv.*, **8**, 6356 (2018)
54. M.Quant, A.Lennartson, A.Dreos, M.Kuisma, P.Erhart, K.Börjesson, K.Moth-Poulsen. *Chem. – Eur. J.*, **22**, 13265 (2016)
55. A.B.Skov, N.Ree, A.S.Gertsen, P.Chabera, J.S.Lissau, L.Nucci, T.Pullerits, K.V.Mikkelsen, M.B.Nielsen, T.I.Sølling, T.Hansen. *ChemPhotoChem*, **3**, 619 (2019)
56. A.Vlasceanu, M.Cacciarini, M.B.Nielsen. *Tetrahedron*, **74**, 6635 (2018)
57. A.U. Petersen, S.L.Broman, S.T.Olsen, A.S.Hansen, L.Du, A.Kadziola, T.Hansen, H.G.Kjaergaard, K.V.Mikkelsen, M.B.Nielsen. *Chem. – Eur. J.*, **21**, 3968 (2015)
58. A.Vlasceanu, S.L.Broman, A.S.Hansen, A.B.Skov, M.Cacciarini, A.Kadziola, H.G.Kjaergaard, K.V.Mikkelsen, M.B.Nielsen. *Chem. – Eur. J.*, **22**, 10796 (2016)
59. A.Vlasceanu, B.N.Frandsen, A.B.Skov, A.S.Hansen, M.G.Rasmussen, H.G.Kjaergaard, K.V.Mikkelsen, M.B.Nielsen. *J. Org. Chem.*, **82**, 10398 (2017)
60. M.Mansø, M.D.Kilde, N.Ree, A.U. Petersen, K.Moth-Poulsen, K.V.Mikkelsen, M.B.Nielsen. *Org. Biomol. Chem.*, **17**, 7735 (2019)